JOURNAL OF THE AMERICAN CHEMICAL SOCIETY

Article

Theoretical Prediction of Noble Gas Containing Anions FNgO (Ng = He, Ar, and Kr)

Tsung-Hui Li, Chun-Hao Mou, Hui-Ru Chen, and Wei-Ping Hu

J. Am. Chem. Soc., **2005**, 127 (25), 9241-9245• DOI: 10.1021/ja051276f • Publication Date (Web): 04 June 2005

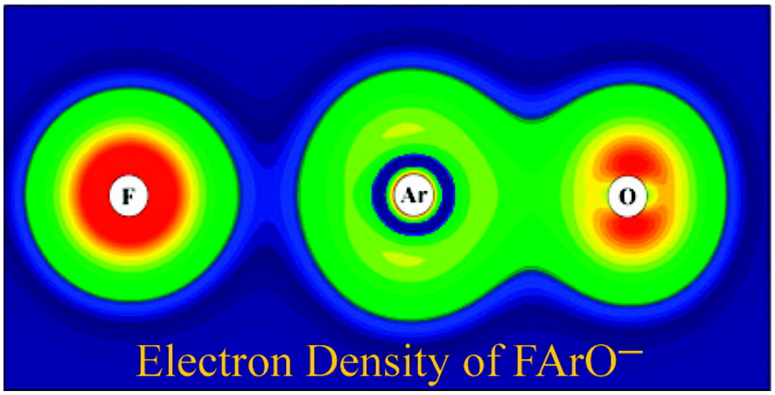

J|A|C|S
ARTICLES
Published on Web 06/04/2005

Theoretical Prediction of Noble Gas Containing Anions $FNgO^-$ (Ng = He, Ar, and Kr)

Tsung-Hui Li, Chun-Hao Mou, Hui-Ru Chen, and Wei-Ping Hu*

Contribution from the Department of Chemistry and Biochemistry, National Chung Cheng University, Chia-Yi, Taiwan 621

Received March 1, 2005; Revised Manuscript Received April 17, 2005; E-mail: chewph@ccu.edu.tw

Abstract: The structures and energies of the noble gas containing anions $FNgO^-$ (Ng = He, Ar, and Kr) have been calculated by high-level ab initio calculations. The $FNgO^-$ anions were found to be deep-energy minima at the singlet electronic state, and their energies are significantly lower than those at the triplet state. High dissociation energy barriers to Ng + OF^- were also predicted. The unexpected stability of the $FNgO^-$ was due to the dramatic ion-induced O=Ng bond formation. The calculated results suggested possible experimental identification of the anionic species and even some related “ionic compounds” under cryogenic conditions.

Introduction

The noble gas elements were discovered in the 1890s by Ramsay and co-workers.[1] Unlike other chemical elements, the noble gases were found to be extremely stable and did not form compounds with other elements. The electronic configuration of the noble gas, or the so-called octet rule, has been used by chemists since early 20th century and by almost every chemistry textbook today to illustrate the principles of chemical bonding. Despite the prediction by some distinguished chemists, including Linus Pauling, that the heavier noble gas elements could combine with other elements to form chemical compounds, all the synthesis attempts were unsuccessful[2] until 1962 when Neil Barlette prepared the first noble gas compound $XePtF_6$.[3] Since then many Xe-containing compounds and the KrF_2 molecule have been experimentally identified.[1] In the past decade, various new noble gas molecules have been successfully prepared and identified in the noble gas matrixes.[4] Most of these molecules are of the HNgY type where Ng is a noble gas atom and Y is an electronegative atom or group. The first Ar-containing neutral molecule HArF was discovered in 2000 by Räsänen and co-workers,[5] and HKrF was identified in 2002 by the same group.[6] The noble gas was also found to form ligands for transition-metal ions[7,8] and to form actinide complexes with CUO molecule.[9]

Since the noble gas atom has “saturated” shells of electrons, it is generally held that the positive charged ions are easier to form than the neutral noble gas molecules, and the negative charged ions would be even less stable. Indeed, cations such as HeH^+ and $HeNe^+$ have been observed in gaseous discharge tubes before the first neutral noble gas compound was discovered. On the other hand, the only known stable noble gas anions were fluorinated or oxygenated Xe ions, and no stable molecular anions of lighter noble gas have been experimentally observed. In the quest of synthesizing ionic compounds of lighter noble gas elements (He, Ne, Ar), stable anions are of crucial importance since the noble gas containing cations would dissociate to neutral noble gas atoms on contact with almost any known anions.[10] From the theoretical point of view, it is also very interesting to know if any special types of electronic structures would allow the formation of stable noble gas containing molecular anions. Some van der Waal complexes between anions and argon have been discussed in the literature but all with very low binding energies.[11,12] In our computational search for stable noble gas molecules and ions, we have recently noticed that the $FNgO^-$ ions (Ng = He, Ar, Kr) have very compact structures and singlet ground states with large singlet−triplet gaps. Thus we have decided to perform high-level ab initio calculation to study the structures and stabilities of these potentially stable noble gas containing molecular anions. The related “ionic” molecules of LiFNgO were also theoretically investigated.

Method

Møller−Plesset second-order perturbation theory (MP2)[13] and the coupled-cluster method CCSD(T)[14] were applied with Dunning’s augmented correlation consistent basis sets (aug-cc-pV*n*Z, *n* = D, T,

---

(1) Greenwood, N. N.; Earnshaw, A. In *Chemistry of the Elements*; Butterworth-Heinemann: Oxford, 2001; p 888.
(2) Laszlo, P.; Schrobilgen, G. J. *Angew. Chem., Int. Ed. Engl.* **1988**, *27*, 479.
(3) Bartlett, N. *Proc. Chem. Soc.* **1962**, 218.
(4) (a) Pettersson, M.; Lundell, J.; Räsänen, M. *J. Chem. Phys.* **1995**, *102*, 6423. (b) Pettersson, M.; Lundell, J.; Räsänen, M. *J. Chem. Phys.* **1995**, *103*, 205. (c) Pettersson, M.; Lundell, J.; Khriachtchev, L.; Räsänen, M. *J. Chem. Phys.* **1998**, *109*, 618.
(5) Khriachtchev, L.; Pettersson, M.; Runeberg, N.; Lundell, J.; Räsänen, M. *Nature* **2000**, *406*, 874.
(6) Pettersson, M.; Khriachtchev, L.; Lignell, A.; Räsänen, M. *J. Chem. Phys.* **2002** *116*, 2508.
(7) Seidel, S.; Seppelt, K. *Science* **2000**, *290*, 117.
(8) Hu, W.-P.; Huang, C.-H. *J. Am. Chem. Soc.* **2001**, *123*, 2340.
(9) (a) Li, J.; Bursten, B. E.; Liang, B.; Andrews, L. *Science* **2002**, *295*, 2242. (b) Andrews, L.; Liang, B.; Li, J.; Bursten, B. E. *J. Am. Chem. Soc.* **2003**, *125*, 3126. (c) Liang, B.; Andrews, L.; Li, J.; Bursten, B. E. *Inorg. Chem.* **2004**, *43*, 882.
(10) Christe, K. O. *Angew. Chem., Int. Ed.* **2001**, *40*, 1419.
(11) Botschwina, P.; Oswald, R. *Chem. Phys. Lett.* **2003**, *377*, 156.
(12) Adamovic, I.; Gordon, M. S. *J. Phys. Chem. A* **2004**, *108*, 11042 and references therein.

10.1021/ja051276f CCC: $30.25

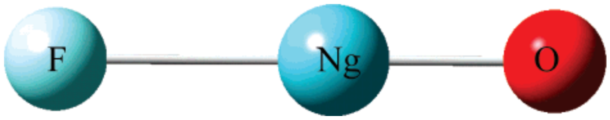

Figure 1. Schematic plot of $F^-\cdots NgO$.

Q)[15] to calculate the structures and energies of the $FNgO^-$ ion (Ng = He, Ar, Kr). The triplet state energies at the singlet-state geometry, the dissociation energies to $F^- + Ng + O$, $F + Ng + O^-$, and $FO^- + Ng$, and the structures and energies of the transition states for the $FO^- + Ng$ dissociation channel were also calculated. The same properties for the possible "ionic" molecules formed by Li cation and $FNgO^-$ were also calculated using aug-cc-pVDZ and aug-cc-pVTZ basis sets. The electronic calculation was performed using the Gaussian 03 program.[16] The geometry optimization methods employed for the stationary points were the Berny[17] and eigenvalue following (EF)[18] methods in the MP2 and CCSD(T) calculation, respectively.

Results and Discussion

The linear $FNgO^-$ ion, as depicted in Figure 1, can be viewed as an ion−dipole complex of $F^-\cdots NgO$. However, unlike a normal ion−dipole complex, the dipole NgO molecule itself is highly unstable. The HeO molecule is not chemically bound, while ArO and KrO do correspond to energy minima on the singlet electronic state. However, at larger Ng−O bond distances, the triplet state, which is purely repulsive, is significantly lower in energy. The triplet state crosses the singlet state at bond distances only slightly longer than the equilibrium bond distance (r_e) on the singlet state. Thus, the singlet ArO or KrO molecule crosses readily into the triplet state during vibration and dissociates into constituent atoms. In the current study, however, we found that the Ng=O bonds can be substantially stabilized in the presence of a fluoride ion. The situation is illustrated in Figure 2 where the singlet and triplet potential-energy curves along the Ar−O distances were plotted for ArO and $FArO^-$. As seen in the Figure, the singlet ArO has a shallow potential-energy well at a bond length of ~1.8 Å. The sharply repulsive triplet state of ArO, however, crosses the singlet state at almost the same bond length. When a fluoride ion is present, however, a significantly deeper energy well occurs at slightly shorter Ar−O distance.

More importantly, the triplet state now crosses at much larger Ar−O distance (~0.3 Å longer than r_e) where the energy is ~7 kcal/mol higher. This deepening of the energy well could make the $FNgO^-$ metastable species and make the experimental identification possible. Similar plots were also obtained for $FHeO^-$ and $FKrO^-$ where the singlet−triplet crossing points are also ~0.3 Å longer than r_e and are ~10 and ~15 kcal/mol, respectively, higher in energies than those at r_e. It is also shown in Figure 2 that in $FArO^-$ the interaction between Ar and O atoms is of much longer range than in ArO.

The calculated bond lengths of $FNgO^-$ were shown in Table 1. As shown in the table, the calculated Ng−O distances are very short and are 1.110, 1.781, and 1.854 Å for Ng = He, Ar, and Kr, respectively, at the CCSD(T)/aug-cc-pVTZ level. The $FNeO^-$ was found to be not an energy minimum. The calculated F−Ng distances are 1.626, 2.241, and 2.259 Å for He, Ar, and Kr, respectively, at the CCSD(T)/aug-cc-pVTZ level, significantly longer than the calculated Ng−O distances. All the calculated $FNgO^-$ structures are linear, and thus they can be suitably represented by the structural formula $F^-\cdots Ng{=}O$. In comparison, the F−Ng distances in HNgF molecules calculated at the same level are 1.415, 1.993, and 2.041 Å for Ng = He, Ar, and Kr, respectively.[19−21] That is, the F−Ng bonds in $FNgO^-$, which are ion−dipole interaction in nature, are only ~0.2 Å longer than the ionic bonding in the neutral HNgF molecule. Interestingly, the calculated F−Ng distances in $FArO^-$ and $FKrO^-$ are almost identical. The calculated relative energies of $FNgO^-$ were listed in Table 2. We will use the energies calculated at the CCSD(T)/aug-cc-pVQZ level for the discussion below unless stated otherwise. As shown in the table, at the singlet-state minimum-energy structure the energies of $FNgO^-$ are significantly lower than those in the triplet state. The S−T energy gaps are 91, 42, and 53 kcal/mol for $FHeO^-$, $FArO^-$, and $FKrO^-$, respectively. This is compared to the energy gaps of 10 and 26 kcal/mol for ArO and KrO, respectively. At the singlet state, three low-energy unimolecular dissociation channels exist for $FNgO^-$: (1) to $F^- + Ng + O$, (2) to $F + Ng + O^-$, and (3) to $FO^- + Ng$. As seen in Table 2, the second channel is ~5 kcal/mol lower in energy than the first channel. Relative to the dissociation products of the second channel, $FNgO^-$ are 16, 34, and 55 kcal/mol lower in energies for Ng = He, Ar, and Kr, respectively. In comparison, the calculated bond energies of ArO and KrO are 9 and 22 kcal/mol. Thus in the presence of the fluoride ion the total bond energies (the energies for the first dissociation channel) increase by 31 and 37 kcal/mol, significantly larger than those in normal ion−dipole complexes. The third channel leads to the global minimum on the singlet-state potential-energy surface. The energies of $FNgO^-$ were found to be 55, 37, and 16 kcal/mol higher than the dissociation products of the third channel for Ng = He, Ar, and Kr, respectively. The transition states for this channel were found to have triangular structures with elongated F−Ng and Ng−O bonds. (The calculated structural parameters are included in the Supporting Information.) Sizable energy barriers of 19, 33, and 50 kcal/mol for Ng = He, Ar, and Kr, respectively, were calculated for this dissociation channel. In comparison, the dissociation barriers of HArF and HKrF to HF and Ar or

---

(13) Møller, C.; Plesset, M. S. *Phys. Rev.* **1934**, *46*, 618.
(14) Raghavachari, K.; Trucks, G. W.; Pople, J. A.; Head-Gordon, M. *Chem. Phys. Lett.* **1989**, *157*, 479.
(15) (a) Dunning Jr., T. H. *J. Chem. Phys.* **1989**, *90*, 1007. (b) Kendall, R. A.; Dunning, T. H., Jr. *J. Chem.* Phys. **1992**, *96*, 6796. (c) Woon, D. E.; Dunning, T. H., Jr. *J. Chem. Phys.* **1993**, *98*, 1358. (d) Wilson, A. K.; Woon, D. E.; Peterson, K. A.; Dunning, T. H., Jr. *J. Chem. Phys.* **1999**, *110*, 7667.
(16) Frisch, M. J.; Trucks, G. W.; Schlegel, H. B.; Scuseria, G. E.; Robb, M. A.; Cheeseman, J. R.; Montgomery, J. A., Jr.; Vreven, T.; Kudin, K. N.; Burant, J. C.; Millam, J. M.; Iyengar, S. S.; Tomasi, J.; Barone, V.; Mennucci, B.; Cossi, M.; Scalmani, G.; Rega, N.; Petersson, G. A.; Nakatsuji, H.; Hada, M.; Ehara, M.; Toyota, K.; Fukuda, R.; Hasegawa, J.; Ishida, M.; Nakajima, T.; Honda, Y.; Kitao, O.; Nakai, H.; Klene, M.; Li, X.; Knox, J. E.; Hratchian, H. P.; Cross, J. B.; Bakken, V.; Adamo, C.; Jaramillo, J.; Gomperts, R.; Stratmann, R. E.; Yazyev, O.; Austin, A. J.; Cammi, R.; Pomelli, C.; Ochterski, J. W.; Ayala, P. Y.; Morokuma, K.; Voth, G. A.; Salvador, P.; Dannenberg, J. J.; Zakrzewski, V. G.; Dapprich, S.; Daniels, A. D.; Strain, M. C.; Farkas, O.; Malick, D. K.; Rabuck, A. D.; Raghavachari, K.; Foresman, J. B.; Ortiz, J. V.; Cui, Q.; Baboul, A. G.; Clifford, S.; Cioslowski, J.; Stefanov, B. B.; Liu, G.; Liashenko, A.; Piskorz, P.; Komaromi, I.; Martin, R. L.; Fox, D. J.; Keith, T.; Al-Laham, M. A.; Peng, C. Y.; Nanayakkara, A.; Challacombe, M.; Gill, P. M. W.; Johnson, B.; Chen, W.; Wong, M. W.; Gonzalez, C.; Pople, J. A. *Gaussian03*, revision C02; Gaussian, Inc.: Wallingford, CT, 2004.
(17) Peng, C.; Ayala, P. Y.; Schlegel, H. B.; Frisch, M. J. *J. Comput. Chem.* **1996**, *17*, 49.
(18) Bannerjee, A.; Adams, N.; Simons, J.; Shepard, R. *J. Phys. Chem.* **1985**, *89*, 52.
(19) Wong, M. W. *J. Am. Chem. Soc.* **2000**, *122*, 6289.
(20) Runeberg, N.; Pettersson, M.; Khriachtchev, L.; Lundell, J.; Räsänen, M. *J. Chem. Phys.* **2001**, *114*, 836.
(21) Chen, Y.-L.; Hu, W.-P. *J. Phys. Chem. A* **2004**, *108*, 4449.

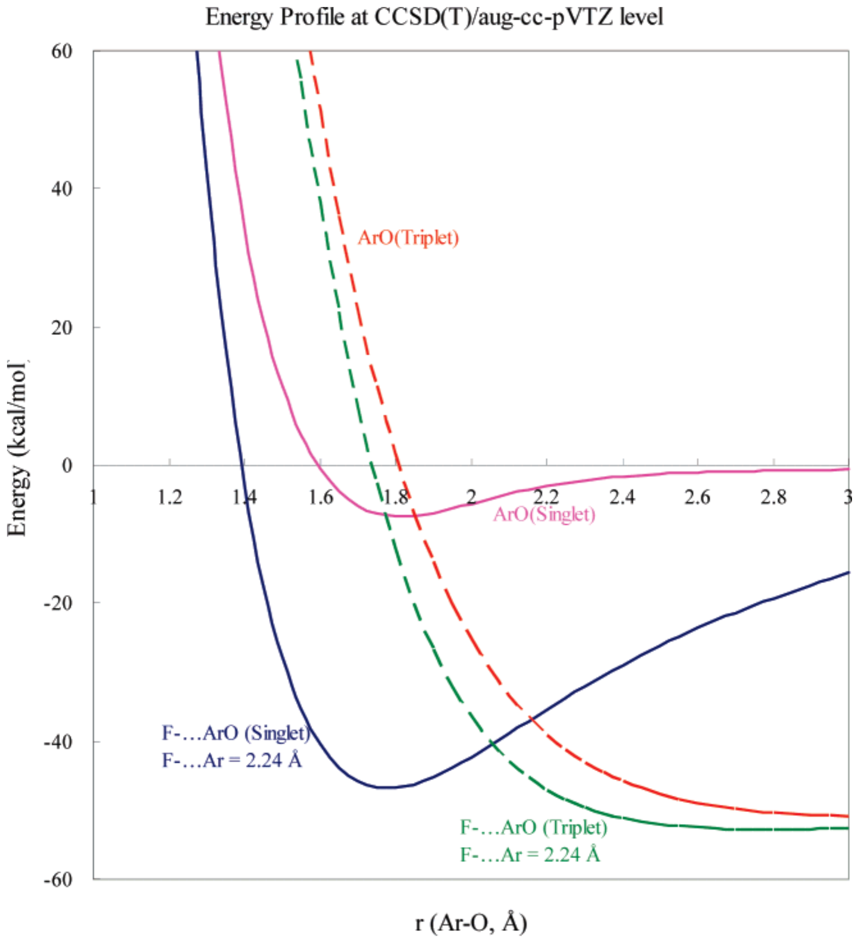

Figure 2. Potential-energy profile of ArO and FArO$^-$. The energies were calculated at the CCSD(T)/aug-cc-pVTZ level. The ArO energies are relative to Ar + O (S) and the FArO$^-$ energies are relative to F$^-$···Ar + O (S) with F−Ar distance fixed at 2.24 Å.

Table 1. Calculated Bond Lengths (Å) of FNgO$^-$ at Various Theoretical Levels

	FHeO$^-$		FArO$^-$		FKrO$^-$	
method	F–He	He–O	F–Ar	Ar–O	F–Kr	Kr–O
MP2/aug-cc-pVDZ	1.637	1.054	2.271	1.729	2.251	1.817
MP2/aug-cc-pVTZ	1.606	1.043	2.214	1.685	2.211	1.786
MP2/aug-cc-pVQZ	1.601	1.038	2.196	1.672	2.198	1.780
CCSD(T)/aug-cc-pVDZ	1.656	1.132	2.280	1.846	2.297	1.903
CCSD(T)/aug-cc-pVTZ	1.626	1.110	2.241	1.781	2.259	1.854
CCSD(T)/aug-cc-pVQZ	1.621	1.100	2.224	1.763		

Kr were calculated to be 24 and 33 kcal/mol, respectively.[22,23] Consequently, the calculated results indicated that at the singlet state, the FNgO$^-$ are dynamically stable from unimolecular dissociation. The lifetime of FNgO$^-$ is then determined by the rate of intersystem crossing to the triplet state. As mentioned earlier, the crossing points were estimated to be 7−15 kcal/mol higher in energies and ∼0.3 Å longer in NgO distances relative to the singlet equilibrium structures. At low temperatures, the rates of intersystem crossing would be limited by the thermal activation to the crossing points. According to transition-state theory, the unimolecular rate constants for thermal activation of 7 kcal/mol should be lower than $\sim10^{-4}$ s^{-1} or a lifetime of $\sim10^4$ s at 70 K. The theoretical lifetimes at even lower temperatures are significantly longer. Furthermore, the energies of FNgO$^-$ at CCSD(T)/aug-cc-pVTZ level are 131, 103, and 100 kcal/mol lower than those of FNgO at the anion geometry for Ng = He, Ar, and Kr, respectively. Thus the autoelectron detachment is an unlikely process. Therefore it seems possible that FNgO$^-$ would be observable as a transient species under cryogenic conditions. Compared to the triplet dissociation limits, F$^-$ + Ng + O (T), Table 2 shows that the energy of FHeO$^-$ and FArO$^-$ are 30 and 10 kcal/mol higher, respectively, but the energy of FKrO$^-$ is 9 kcal/mol *lower*. It is evident that the calculated relative energies in Table 2 have not converged with respect to the basis set sizes. Thus, in Table 2 we also used a simple extrapolation method[24] based on the CCSD(T) energies calculated with aug-cc-pVnZ (n = D, T, Q) basis sets to estimate the relative energies at the complete basis set (CBS) limit. The differences between the CCSD(T)/CBS and the CCSD(T)/aug-cc-pVQZ values, <1 kcal/mol for the barrier heights and <4 kcal/mol for dissociation energies, are reasonable estimations of the error bars for the calculated relative energies.

Table 3 shows the calculated harmonic vibrational frequencies and IR intensities of FNgO$^-$. Both the Ng═O and Ng−F stretching modes were predicted to show strong IR signals. It is also interesting to note that the Kr−F stretching frequency was predicted to be 20−30 cm^{-1} higher than the Ar−F frequency. Table 4 shows the calculated atomic charges for FNgO$^-$. Large charge separations were assigned at the O═Ng

---

(22) Chaban, G. M.; Lundell, J.; Gerber, R. B. *Chem. Phys. Lett.* **2002**, *364*, 628.
(23) Yen, S.-Y.; Mou, C.-H.; Hu, W.-P. *Chem. Phys. Lett.* **2004**, *383*, 606.
(24) Feyereisen, M. W.; Feller, D.; Dixon, D. A. *J. Phys. Chem.* **1996**, *100*, 2993.

Table 2. Calculated Relative Energies[a] (kcal/mol) of $FNgO^-$

	S–T gap[b]	relative to $F^- + Ng + O$ (S)	relative to $F^- + NgO$	relative to $F + Ng + O^-$	relative to $F^- + Ng + O$ (T)	relative to $FO^- + Ng$	barrier[c]
			Ng = He				
MP2/aug-cc-pVTZ	118.0	−31.8	NA	−17.0	34.3	56.5	29.0 [25.0][e]
MP2/aug-cc-pVQZ	121.3	−32.9	NA	−19.1	32.2	55.8	29.9 [26.0]
CCSD(T)/aug-cc-pVTZ	86.6	−19.2	NA	−14.1	31.6	55.3	17.7 [14.4]
CCSD(T)/aug-cc-pVQZ	90.8	−20.5	NA	−15.9	29.8	54.8	19.0
CCSD(T)/CBS[f]	91.1	−20.4	NA	−16.4	29.6	54.7	19.3
			Ng = Ar				
MP2/aug-cc-pVTZ	61.0	−51.4	−31.1	−36.6	14.7	36.8	44.6 [43.0]
MP2/aug-cc-pVQZ	65.6	−53.7	−31.8	−30.5	23.0	35.0	46.6 [45.0]
CCSD(T)/aug-cc-pVTZ	38.0	−37.1	−29.7	−32.0	13.7	37.4	31.9 [30.6]
CCSD(T)/aug-cc-pVQZ	42.2	−40.4	−31.9	−34.1	9.9	36.5	33.1[g]
CCSD(T)/CBS	41.9	−42.5	−34.0	−34.9	7.5	36.2	33.4
			Ng = Kr				
MP2/aug-cc-pVTZ	72.2	−76.0	−35.9	−61.2	−9.9	12.2	65.5 [64.0]
MP2/aug-cc-pVQZ	74.4	−77.8	−39.9	−64.0	−12.7	10.9	66.9 [65.4]
CCSD(T)/aug-cc-pVTZ	52.7	−58.1	−37.4	−52.9	−7.3	16.4	49.0[h]
CCSD(T)/aug-cc-pVQZ[g]	52.8	−59.3	−37.7	−54.7	−9.0	15.9	50.4[h]
CCSD(T)/CBS	52.4	−60.0	−41.0	−52.3	−10.0	18.7	49.7

[a] Born−Oppenheimer energies, not including zero-point vibrational energies. [b] Energy differences between the singlet and the triplet state at the optimized singlet-state geometry. [c] Energy barriers for the $FNgO^- \rightarrow FO^- + Ng$ reactions. [d] Not applicable. [e] Values in parentheses including vibrational zero-point energies. [f] Extrapolated results to the complete basis set limit, see text. [g] Single-point energy at CCSD(T)/aug-cc-pVTZ structure except for the barrier. [h] Single-point energy at CCSD(T)/aug-cc-pVDZ structure.

Table 3. Calculated Harmonic Vibrational Frequencies (cm^{-1}) of $FNgO^-$ at Two Theoretical Levels

	MP2/aug-cc-pVTZ	CCSD(T)/aug-cc-pVTZ
υ_{He-O}	1692 (183)[a]	1273
υ_{F-He-O}	508 (35)	449
υ_{He-F}	350 (116)	331
υ_{Ar-O}	743 (192)	535
υ_{F-Ar-O}	197 (37)	175
υ_{Ar-F}	271 (69)	275
υ_{Kr-O}	713 (130)	539
υ_{F-Kr-O}	192 (40)	170
υ_{Kr-F}	304 (234)	294

[a] Values in parentheses are calculated IR intensities (in Km/mol).

Table 4. Calculated Atomic Charges[a]

	F	Ng	O
$FHeO^-$	−0.83 (−0.91)	0.43 (0.57)	−0.60 (−0.66)
$FArO^-$	−0.83 (−0.94)	0.49 (0.86)	−0.66 (−0.92)
$FKrO^-$	−0.78 (−0.85)	0.52 (0.86)	−0.75 (−1.01)

[a] By ChelpG and NBO (in parentheses) methods using electron density calculated at MP2/aug-cc-pVTZ level, in atomic unit, *e*.

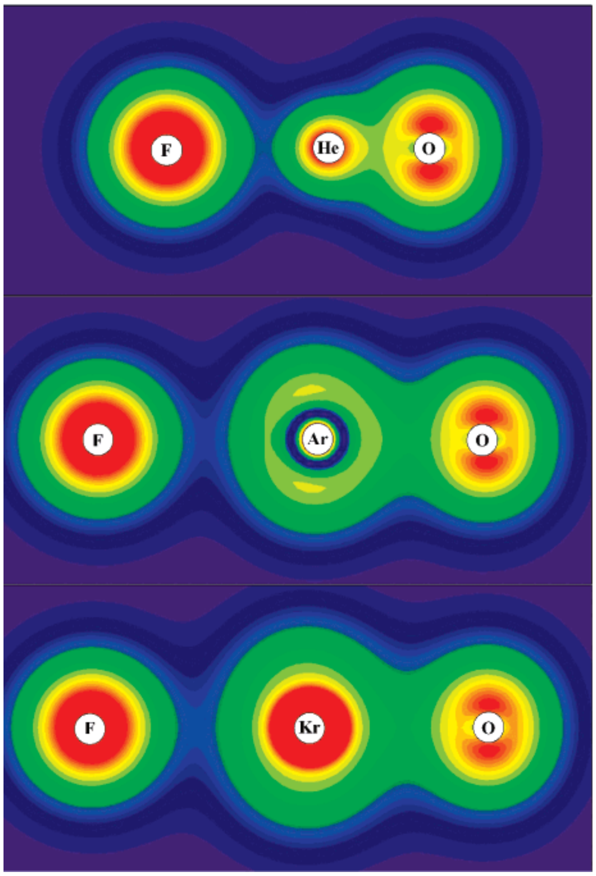

Figure 3. Contour plots of the calculated electron density (MP2/aug-cc-pVTZ level) of $FHeO^-$, $FArO^-$, and $FKrO^-$.

bonds. The fluorine atoms were predicted to retain almost the entire negative charges. This is consistent with the picture of the anion-induced formation of the polar Ng═O bonds mentioned earlier. Figure 3 shows the contour plots of the calculated electron density. The negligible distortion of the concentric electron density around the fluorine atoms shows the retention of the anionic character while the electron density distribution between the noble gas and the oxygen atoms suggests the highly polar Ng═O bonds.

If the $FNgO^-$ are stable anions, can they combine with cations to form “ionic compounds”? We explore this possibility by calculating the structures and relative energies of LiFNgO molecules. Figure 4 shows the calculated structures of LiFArO and LiFKrO at the CCSD(T)/aug-cc-pVTZ level. Detailed geometry parameters and relative energies are included in the Supporting Information. The calculated structure of LiFArO is planar with two parallel aligned dipoles while the calculated structure of LiFKrO is linear. The following discussion will be based on the calculated results at the CCSD(T)/aug-cc-pVTZ level.

Compared to the structures of $FNgO^-$, the Ng═O bonds in LiFArO and LiFKrO are slightly shorter (~0.02 Å) and the Ng−F distances are significantly longer (0.4−0.6 Å). At the singlet minimum structures, the singlet states are more stable than the triplet states with S−T gaps of 24 and 37 kcal/mol for

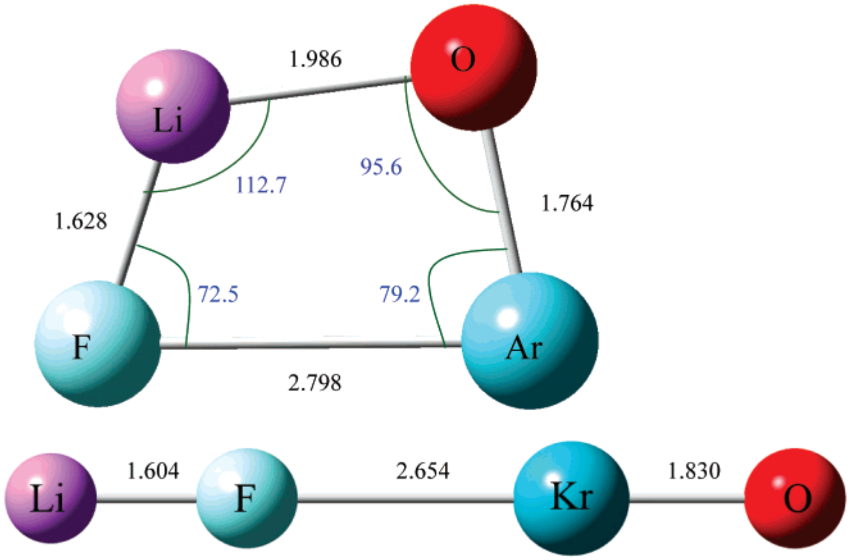

Figure 4. The calculated structures of LiFArO and LiFKrO. Bond lengths are in angstroms and bond angles in degrees.

LiFArO and LiFKrO, respectively. The calculated energies of LiFArO and LiFKrO are 172 and 155 kcal/mol below those of $Li^+ + FNgO^-$. Alternatively, the energies of LiFArO and LiFKrO are 20 and 11 kcal/mol lower than the sum of LiF and ArO or KrO. These are significantly stronger than normal dipole–dipole interactions. Similar to the case of $FNgO^-$, the global minima on the singlet surfaces for the LiFNgO systems are LiOF + Ng. The energies of LiFArO and LiFKrO were calculated to be 37 and 33 kcal/mol higher than the global minima and the corresponding energy barriers for dissociation were calculated to be ~17 kcal/mol. The LiFHeO was found to have negligible dissociation barrier to the global minimum and is thus not dynamically stable.

Summary

The current study shows that the unstable Ng═O bonds can be strengthened considerably in the presence of a fluoride ion. The $FNgO^-$ were predicted to be tightly binding anions and were predicted to have large S–T gaps and high unimolecular dissociation energy barriers. From the theoretical point of view, the special chemical bonding in $FNgO^-$, the anion-induced strong Ng═O formation, is very unique and interesting. Although it is difficult to predict whether $FNgO^-$ can actually be synthesized and observed, the calculated results did suggest that, in suitable environments, possibly under cryogenic conditions in solid noble gas matrixes or in molecular beams, the $FNgO^-$ anions may have a chance to be experimentally identified.

Acknowledgment. This work is supported by the National Science Council of Taiwan, Grant no. NSC 93-2113-M-194-002. We are grateful to the National Center for High-Performance Computing (NCHC) of Taiwan for providing part of the computational resources.

Supporting Information Available: Tables of calculated geometry, relative energies, vibrational frequencies, atomic charges, figures of potential energy profiles (PDF). This material is available free of charge via the Internet at http://pubs.acs.org.

JA051276F